

## Characterization of ATP and P<sub>2</sub> agonists binding to the cardiac plasma membrane P<sup>1</sup>,P<sup>4</sup>-diadenosine 5'-tetrphosphate receptor

Grant E. Blouse <sup>a</sup>, Guang Liu <sup>b</sup>, Richard H. Hilderman <sup>c,\*</sup>

<sup>a</sup> Department of Biochemical Research, Henry Ford Health System, Detroit, MI 48202-2689, USA

<sup>b</sup> Department of Neuroscience, Tufts University School of Medicine, Boston, MA 02111, USA

<sup>c</sup> Departments of Microbiology/Molecular Medicine, Biological Sciences, Vascular Research Laboratory, Greenville Hospital System/Clemson University Biomedical Cooperative and the South Carolina Experiment Station, Clemson University, Clemson, SC 29634-1903, USA

Received 11 May 1998; revised 16 July 1998; accepted 16 July 1998

### Abstract

P<sup>1</sup>,P<sup>4</sup>-Diadenosine 5'-tetrphosphate (Ap<sub>4</sub>A) acts as an extracellular modulator through its interaction with purinoceptors. Our laboratory has demonstrated the presence of an Ap<sub>4</sub>A receptor in cardiac tissue [1,2]. Due to the rapid hydrolysis of ATP by cardiac membranes the relationship of ATP and Ap<sub>4</sub>A binding to purinoceptors on cardiac membranes has not been characterized. In this communication we used two approaches to determine the relationship of ATP to the Ap<sub>4</sub>A receptor. Radioligand binding carried out with [α-<sup>32</sup>P]Ap<sub>4</sub>A and adenosine 5'-O-[3-thiotriphosphate] ([γ-<sup>35</sup>S]ATPγS) demonstrates the presence of a single high affinity binding site for Ap<sub>4</sub>A and the presence of two binding sites for ATPγS.

The second approach utilized immunoaffinity purified Ap<sub>4</sub>A receptor that was shown to be free of ATPase and Ap<sub>4</sub>Aase activities. Non-radiolabeled Ap<sub>4</sub>A and ATPγS effectively inhibited photocrosslinking of [α-<sup>32</sup>P]8-N<sub>3</sub>Ap<sub>4</sub>A to the receptor polypeptide while ATP was a much less effective inhibitor. Furthermore, on plasma membranes [α-<sup>32</sup>P]8-N<sub>3</sub>Ap<sub>4</sub>A photocrosslinked to only a 50 kDa polypeptide. These data are consistent with Ap<sub>4</sub>A interacting with a homogeneous population of receptors on cardiac plasma membranes but with ATP having a low affinity for the receptor. © 1998 Elsevier Science B.V. All rights reserved.

**Keywords:** Ap<sub>4</sub>A receptor; ATPγS; ATP; Anti-Ap<sub>4</sub>A receptor monoclonal antibody

### 1. Introduction

In recent years it has become increasingly clear that adenylated dinucleotides act as extracellular modulators of various biological processes. P<sup>1</sup>,P<sup>4</sup>-Diadenosine 5'-tetrphosphate (Ap<sub>4</sub>A) is one of the most abundant and the best characterized adenylated

dinucleotide. Ap<sub>4</sub>A is co-stored with Ap<sub>3</sub>A, Ap<sub>5</sub>A, Ap<sub>6</sub>A and ATP in the dense secretory granules of platelets [3,4]. In chromaffin cells, Ap<sub>4</sub>A, Ap<sub>5</sub>A, Ap<sub>6</sub>A are co-stored with AMP, ADP, ATP and catecholamines [5,6]. It has been estimated that following localized release from platelets and chromaffin cells, Ap<sub>4</sub>A could reach physiologically significant concentrations. Furthermore, compared with ATP, Ap<sub>4</sub>A has a relatively long half-life in whole blood [7]. Thus, Ap<sub>4</sub>A is well suited for a role as an extracellular modulator.

\* Corresponding author. Fax: (864) 6560435;  
E-mail: hilderr@clemson.edu

Among the better characterized targets for extracellular  $\text{Ap}_4\text{A}$  are cells of the vascular system.  $\text{Ap}_4\text{A}$  has been shown to modulate blood vessel tone [8–10], induce the release of nitric oxide from endothelial cells [11], prime respiratory burst and regulate apoptosis in neutrophils [12] and inhibit ADP-induced platelet aggregation [13,14]. Additionally, in other tissues  $\text{Ap}_4\text{A}$  has been shown to promote catecholamine release [15], activate glycogen phosphorylase in hepatocytes [16] and elicit smooth muscle contractions in vas deferens [17] and urinary bladder [18].

The biological effects of  $\text{Ap}_4\text{A}$  on cells have been attributed to its interaction with cell surface receptors where it induces calcium mobilization [19,20]. However, the nature of the receptor(s) in  $\text{Ap}_4\text{A}$  mediated signal transduction remains unclear. In liver plasma membranes  $\text{Ap}_4\text{A}$  appears to bind to a single class of  $\text{P}_{2Y}$  binding sites [21]. In vas deferens and urinary bladder  $\text{Ap}_4\text{A}$  interacts with  $\text{P}_{2X}$  receptors [17,18]. However, in brain synaptosomes  $\text{Ap}_4\text{A}$  interacts with two classes of binding sites: a high affinity site which appears to be specific for adenylylated dinucleotides ( $\text{P}_{2D}$ ) and a second low affinity site [22].

Our laboratory has demonstrated in partially purified cardiac membrane homogenates that  $\text{Ap}_4\text{A}$  interacts with a  $\text{P}_{2D}$  receptor and that this receptor undergoes an activation step which enhances only  $\text{Ap}_4\text{A}$  binding [1,2,23]. In addition, investigators have recently demonstrated in cardiac tissue the existence of  $\text{P}_{2X}$  and  $\text{P}_{2Y}$  purinoceptors [24,25]. These data suggest that  $\text{Ap}_4\text{A}$  may interact with a heterogeneous population of receptors in cardiac tissue that may consist of specific dipurinoceptors and/or one or more  $\text{P}_2$  purinoceptor subtypes. These considerations led us to investigate the relationship of ATP and  $\text{Ap}_4\text{A}$  binding on purified plasma membranes. In this communication we demonstrate that  $\text{Ap}_4\text{A}$  interacts with a homogeneous population of receptors on cardiac plasma membranes while ATP does not bind in appreciable amounts to the  $\text{Ap}_4\text{A}$  receptor.

## 2. Materials and methods

### 2.1. Materials

Swiss mice were obtained from Charles River Lab-

oratories. The animals were housed in an animal facility maintained with a photoperiod of 15L:9D and room temperatures of 22–25°C.  $[\alpha\text{-}^{32}\text{P}]\text{ATP}$  (3000 Ci/mmol) and  $[\text{P}^{32}]\text{inorganic phosphate}$  (3000 Ci/mmol) were purchased from DuPont New England Nuclear.  $[\gamma\text{-}^{35}\text{S}]\text{ATP}\gamma\text{S}$  (1000 Ci/mmol) was purchased from ICN. All nucleotides and goat serum were purchased from Sigma.  $\text{En}^3\text{Hance Spray}$  was obtained from DuPont New England Nuclear. Affi-Gel Hz resin, and Kaleidoscope molecular weight markers were purchased from Bio-Rad. DC-Plastik-folien 20×20 cm PEI-Cellulose F plates were purchased from EM Science. All other reagents were of analytical reagent grade or better.

### 2.2. Synthesis and purification of $[\alpha\text{-}^{32}\text{P}]\text{Ap}_4\text{A}$ and $[\alpha\text{-}^{32}\text{P}]\text{8-N}_3\text{Ap}_4\text{A}$

$[\alpha\text{-}^{32}\text{P}]\text{Ap}_4\text{A}$  and  $[\alpha\text{-}^{32}\text{P}]\text{8-N}_3\text{Ap}_4\text{A}$  were synthesized and purified with yields of about 45% as described [1]. Purity was greater than 95% as determined by thin-layer chromatography and autoradiography.

### 2.3. Purification of cardiac plasma membranes

Mouse cardiac plasma membranes were purified as described [26]. Briefly, four mouse hearts were suspended in 40 vols. of HEPES buffered saline with glucose and potassium (HBSGK), which contained 20 mM HEPES (pH 7.4), 150 mM NaCl, 2 mM glucose, 3 mM KCl and 1 mM  $\text{CaCl}_2$  in addition to 0.1% Triton X-100. The suspended hearts were minced and homogenized with a Dounce homogenizer. After homogenization, the samples were filtered through cheesecloth and centrifuged at  $12\,000\times g$  for 10 min at 4°C. The supernatant was centrifuged at  $100\,000\times g$  for 90 min at 4°C and the pellet was resuspended in 0.5 ml of HBSGK buffer containing 0.1% Triton X-100 and 8.5% sucrose (postmitochondrial membrane).

Plasma membranes were separated from sarcoplasmic reticulum by sucrose density centrifugation of the postmitochondrial membrane fraction. Linear sucrose gradients were formed using 19.5 ml of 62.8% sucrose in HBSGK buffer containing 0.1% Triton X-100 and 9.5 ml of 8.5% sucrose HBSGK buffer containing 0.1% Triton X-100. The samples were

centrifuged in a VTi50 rotor at  $95416\times g$  for 6 h at 4°C. The plasma membrane fraction was identified using membrane marker enzymes as described [26]. The plasma membranes were stored in aliquots at –80°C for up to 3 months without loss of Ap<sub>4</sub>A binding activity.

#### 2.4. Stability of Ap<sub>4</sub>A, ATP, ATPγS and α,β-MeATP during binding assays

All experiments were performed in triplicate and repeated three times. Assays were performed in 0.1 ml reaction mixtures. Reaction mixtures contained either 0.9 μM [α-<sup>32</sup>P]ATP (specific activity 5000–6000 cpm/pmole), 0.5 μM [α-<sup>32</sup>P]Ap<sub>4</sub>A (specific activity 5000–6000 cpm/pmole), 0.6 μM [γ-<sup>35</sup>S]ATPγS (specific activity 30 000–40 000 cpm/pmole) or 0.9 μM [2,8-<sup>3</sup>H]α,β-MeATP (specific activity 3000–4000 cpm/pmole) in 67 mM Tris-HCl, pH 7.7 and 0.1 mM MgCl<sub>2</sub> (assay buffer). The reactions were initiated by the addition of 2.5 μg of plasma membranes and incubated for various times at 20°C. After incubation, 2 μl of the reaction mixture along with 2 μl non-radiolabeled standards (25 mM of Ap<sub>4</sub>A, ATP, ADP, AMP) and [<sup>32</sup>P]inorganic phosphate ( $1.0\times 10^5$  cpm) were spotted on DC-Plastikfolien PEI-Cellulose F Plates (TLC plates).

For experiments involving [α-<sup>32</sup>P]ATP or [α-<sup>32</sup>P]Ap<sub>4</sub>A, TLC plates were developed in 1 M LiCl as described [27]. After development, plates were dried and autoradiography was carried out at –80°C for 4–5 h using Kodak X-OMATAR X-ray film and Cronex Lighting Plus intensifying screens. TLC chromatography with [γ-<sup>35</sup>S]ATPγS was accomplished using 0.3 M K<sub>2</sub>HPO<sub>4</sub>, pH 7.0. Autoradiography was carried out at –80°C for 5 h after spraying TLC plates with En<sup>3</sup>Hance Spray. TLC chromatography with [2,8-<sup>3</sup>H]α,β-MeATP was carried out in 1 M LiCl as described [27]. Autoradiography was carried out at –80°C for 72–96 h after spraying the TLC plates with En<sup>3</sup>Hance Spray.

Densitometer tracings of autoradiographs were obtained using a Pharmacia LKB UltraScan XL Enhanced Laser Densitometer connected to an IBM 486 Personal Computer with LKB GelScan XL (version 2.1) software. Percentage of nucleotide hydrolysis was calculated from the relative percentage of total absorbance units ( $A_{533}\times\text{mm}^2$ ).

#### 2.5. Radionucleotide binding assays

All experiments were performed in triplicate and repeated at least three times. Ap<sub>4</sub>A binding assays were performed as described [28]. Binding assays were performed in 0.1 ml reaction mixtures. Each reaction mixture contained 67 mM Tris-HCl, pH 7.7 and 0.1 mM MgCl<sub>2</sub> (assay buffer) and 0.5 μM [<sup>32</sup>P]Ap<sub>4</sub>A (5000–6000 cpm/pmole). Reactions were initiated by the addition of 2.5 μg of plasma membrane and incubated for 15 min at 20°C. Membranes were collected on Whatman R/A glass fiber discs, washed three times with 3 ml portions of 67 mM Tris-HCl, pH 7.7, 0.1 mM MgCl<sub>2</sub>. The discs were dried and counted in 5 ml of a toluene-based scintillation fluid. Blanks contained all components except membranes.

ATPγS binding was assayed as above except using 0.9 μM [γ-<sup>35</sup>S]ATPγS (5000–6000 cpm/pmole). Due to non-specific binding of [γ-<sup>35</sup>S]ATPγS to the glass fiber discs, the glass fiber discs were presoaked in 67 mM Tris-HCl (pH 7.7) and 50 mM sodium pyrophosphate. Membranes were then collected on these discs, washed three times with 3 ml portions of 67 mM Tris-HCl, pH 7.7, 0.1 mM MgCl<sub>2</sub> and 10 μM sodium pyrophosphate. The discs were dried and counted in 5 ml of a toluene-based scintillation fluid. Blanks contained all components except membranes.

#### 2.6. Computer analysis of binding data

Saturation binding curves were fitted by a weighted non-linear least square method directly to cpm data and analyzed by the program LIGAND [29]. For displacement experiments, all displacement data were fitted simultaneously by LIGAND. This approach involves a multistep weighted non-linear least squares analysis of single homologous, then heterologous displacement data for each radioligand and finally a simultaneous analysis of all displacement data. This approach yields a more reliable estimation of equilibrium binding parameters for multiple ligands [29]. One, two, and three site models were investigated and compared by the *F*-test with the more complex model accepted only if there was a significant reduction in the sum of squares ( $P < 0.05$ ).

## 2.7. Immunoaffinity purification of the $A_{p4A}$ receptor

The Affi-Gel Hz Immunoaffinity Kit (Bio-Rad) was used to generate an anti- $A_{p4A}$  receptor monoclonal antibody (mAb TL4) affinity column. Monoclonal antibody TL4 which blocks  $A_{p4A}$  binding to its cardiac membrane receptor was isolated as described [23]. Monoclonal antibody TL4 (4–5 mg) was exchanged into the coupling buffer (pH 5.5) using an Econ-Pac 10DG desalting column. Monoclonal antibody TL4 carbohydrates were then oxidized in sodium *m*-periodate (20.8 mg/ml) by incubating the sample in the dark for 1 h at room temperature (1:10  $NaIO_4$ :mAb TL4 v/v) followed by desalting through an Econ-Pac 10DG desalting column. Oxidized mAb TL4 was coupled to 3 ml of Affi-Gel Hz resin for 24 h at room temperature in coupling buffer. The mAb TL4 coupled resin (Affi-Gel Hz) was washed with 3 bed vols. of PBS (0.145 M NaCl, 38 mM  $Na_2HPO_4$ , 11 mM  $NaH_2PO_4$ , pH 7.0) containing 0.5 M NaCl and then stored in TBS (50 mM Tris-HCl and 150 mM NaCl, pH 7.4) containing 0.02%  $NaN_3$ .

To immunoaffinity purify the  $A_{p4A}$  receptor the mAb TL4 coupled Affi-Gel Hz resin was blocked by first washing with TBS containing 5% goat serum followed by incubating with TBS containing 20% goat serum overnight at 4°C. Postmitochondrial membrane pellets were resuspended in TBS containing 1% SDS to give a protein concentration of 2 mg/ml. The sample was denatured by boiling for 25 min and then sufficient TBS was added to reduce the SDS to 0.2%. The sample was centrifuged at  $16\,000\times g$  for 30 min and the supernatant incubated overnight at 4°C with mAb TL4 coupled Affi-Gel Hz resin which has been blocked with goat serum. This mixture was packed into a 1.2 cm by 14.5 cm column and washed with 25 ml of TBS. The unbound protein was washed off with 10 mM  $KH_2PO_4$ , pH 6.8 until the  $A_{280}$  was below 0.01. The bound protein was eluted with 200 mM glycine, pH 2.5 in 2.0 ml fractions and the pH of each fraction was neutralized by the addition of 175  $\mu$ l of 1.5 mM Tris-HCl, pH 8.8. The protein eluted as a single  $A_{280}$  peak and the three tubes with highest absorbance were pooled, dialyzed against three changes of 67 mM Tris-HCl (pH 7.7), concentrated by Centricon-10 (Amicon), and stored at  $-20^\circ\text{C}$ . A protease inhibitor cocktail containing leu-

peptin, antipain, chymostatin, pepstatin each at a final concentration of 1  $\mu$ g/ml and 2 mM phenylmethylsulfonyl fluoride was included in all buffers used in the immunoaffinity purification of the  $A_{p4A}$  receptor.

## 2.8. Photolabeling of the immunoaffinity purified receptor

All operations involving 8-azido nucleotides were performed under subdued light. Reaction mixtures contained 5  $\mu$ g of immunoaffinity purified receptor in 30  $\mu$ l of assay buffer plus  $[\alpha\text{-}^{32}\text{P}]\text{8-N}_3\text{Ap}_4\text{A}$  (specific activity 1200–1800 cpm/pmole). These reaction mixtures were incubated for 30 min at 20°C in the dark. The samples were irradiated at 4°C using a short-wavelength UV lamp at 254 nm and a dose rate of 300  $\mu\text{W}/\text{cm}^2$  for 60 s. SDS-PAGE and Western transfer were performed as described [1]. Autoradiography was carried out at  $-80^\circ\text{C}$  for 14–24 h using Kodak X-OMATAR X-ray film and Cronex Lighting Plus intensifying screens. Densitometer analysis of autoradiographs was performed as described above.

## 2.9. Protein determination

Protein concentrations were determined by the Bradford method [30].

# 3. Results

## 3.1. Stability of $A_{p4A}$ and ATP during binding assays

Prior to performing binding experiments it is necessary to ensure that the radiolabeled ligands are not hydrolyzed by plasma membrane nucleases under binding conditions. As shown in Fig. 1,  $[\alpha\text{-}^{32}\text{P}]\text{ATP}$  is rapidly hydrolyzed with only 64.9% and 33.3% of the radiolabel remaining as ATP after 3 and 15 min of incubation, respectively. In contrast,  $[\alpha\text{-}^{32}\text{P}]\text{Ap}_4\text{A}$  and  $[\gamma\text{-}^{35}\text{S}]\text{ATP}\gamma\text{S}$  were significantly more stable with 80% and 92% of the radiolabel remaining intact after 15 min, respectively (Fig. 1). Furthermore, essentially none of the  $[\text{H}]\alpha,\beta\text{-MeATP}$  was hydrolyzed after 60 min (data not shown). Control samples contained all assay components except plasma membranes and

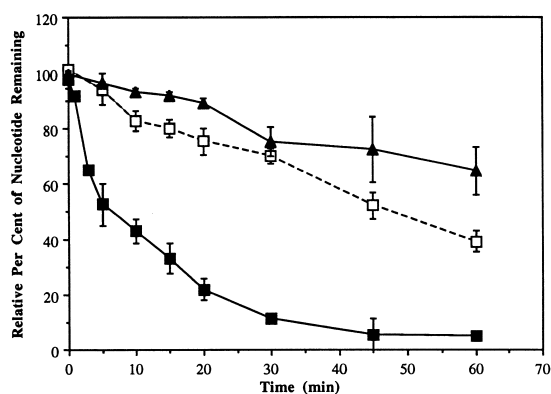


Fig. 1. Time course of nucleotide hydrolysis by cardiac plasma membranes. 2.5  $\mu$ g of plasma membranes were incubated at 20°C in a final volume of 0.1 ml of binding buffer for the indicated times with 0.9  $\mu$ M [ $\alpha$ - $^{32}$ P]ATP (specific activity 5000–6000 cpm/pmole), 0.5  $\mu$ M [ $\alpha$ - $^{32}$ P]Ap<sub>4</sub>A (specific activity 5000–6000 cpm/pmole) or 0.6  $\mu$ M [ $\gamma$ - $^{35}$ S]ATPγS (specific activity 30 000–40 000 cpm/pmole) for the indicated times. After incubations, 2  $\mu$ l of the reaction mixture was spotted on TLC plates and separated as described in Section 2. □, Ap<sub>4</sub>A; ■, ATP; ▲, ATPγS. The relative percentage was calculated from densitometer tracings of autoradiographs as described in Section 2. The results are expressed as averages of three different experiments in triplicate (nine total data points). Error bars are shown as standard deviations.

were incubated for 60 min prior to TLC. No degradation of the radiolabeled nucleotides was detected in these samples. These data are consistent with purified cardiac plasma membranes containing nucleases which rapidly hydrolyze ATP while hydrolyzing Ap<sub>4</sub>A, ATPγS and  $\alpha,\beta$ -MeATP at significantly slower rates.

### 3.2. Binding characteristics of Ap<sub>4</sub>A and ATPγS to cardiac plasma membranes

Due to the rapid hydrolysis of ATP, this ligand was not used in binding studies. The binding of 0.5  $\mu$ M [ $\alpha$ - $^{32}$ P]Ap<sub>4</sub>A to cardiac membranes was linear with protein concentrations from 1.0  $\mu$ g to 4.0  $\mu$ g while the binding of 0.9  $\mu$ M [ $\gamma$ - $^{35}$ S]ATPγS was linear with protein concentrations from 1.0  $\mu$ g to 25.0  $\mu$ g (data not shown). Ap<sub>4</sub>A binding to 2.5  $\mu$ g of plasma membranes reached a plateau after 12 min. Longer incubations up to 30 min did not significantly increase the maximal amount of [ $\alpha$ - $^{32}$ P]Ap<sub>4</sub>A bound (data not shown). [ $\gamma$ - $^{35}$ S]ATPγS binding to 2.5  $\mu$ g cardiac plasma membranes reached a plateau after

10 min. Incubations up to 30 min did not significantly increase the maximal amount of [ $\gamma$ - $^{35}$ S]ATPγS bound (data not shown). These results demonstrated that binding equilibrium was attained within a time where hydrolysis would not be a factor. All subsequent Ap<sub>4</sub>A and ATPγS binding experiments were performed using 2.5  $\mu$ g of plasma membrane for 15 min at 20°C.

### 3.3. Specificity of Ap<sub>4</sub>A and ATPγS binding to cardiac plasma membranes

In an attempt to determine binding parameters for Ap<sub>4</sub>A and ATPγS, binding experiments were performed using a variable amount of either [ $\alpha$ - $^{32}$ P]Ap<sub>4</sub>A or [ $\gamma$ - $^{35}$ S]ATPγS and a fixed amount of plasma membrane (Fig. 2). [ $\alpha$ - $^{32}$ P]Ap<sub>4</sub>A binding plateaued at 0.25  $\mu$ M while [ $\gamma$ - $^{35}$ S]ATPγS plateaued at 0.6  $\mu$ M. Binding data are displayed in the Scatchard coordinate system and indicated a linear relationship for Ap<sub>4</sub>A (Fig. 3A) which suggests that there is a single binding site for Ap<sub>4</sub>A. Data analysis with the program LIGAND is consistent with one class of high affinity binding sites for Ap<sub>4</sub>A with an apparent receptor density ( $B_{\max}$ ) of 66 pmoles mg<sup>-1</sup> of membrane protein and an apparent  $K_d$  value of 0.05  $\mu$ M (Table 1). On the other hand, Scatchard analysis

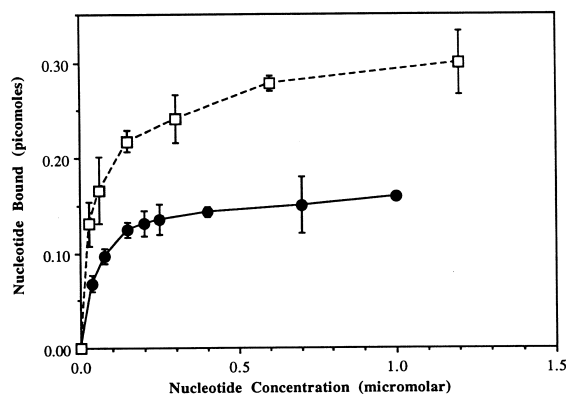


Fig. 2. [ $\alpha$ - $^{32}$ P]Ap<sub>4</sub>A and [ $\gamma$ - $^{35}$ S]ATPγS binding to cardiac plasma membranes. The binding assay is described in the text. Varying concentrations of [ $\alpha$ - $^{32}$ P]Ap<sub>4</sub>A (specific activity 6000–9000 cpm/pmole) or [ $\gamma$ - $^{35}$ S]ATPγS (specific activity 6000–9000 cpm/pmole) were incubated with 2.5  $\mu$ g of plasma membranes for 15 min at 20°C. ●, Ap<sub>4</sub>A; □, ATPγS. The results are expressed as averages of three different experiments performed in triplicate (nine total data points). Error bars are shown as standard deviations.

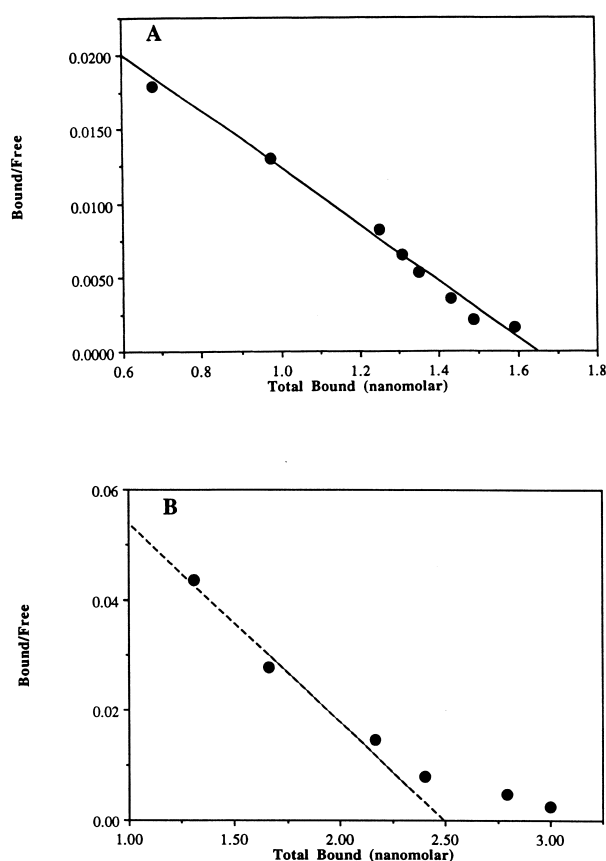


Fig. 3. Scatchard analysis of  $[\alpha\text{-}^{32}\text{P}]\text{Ap}_4\text{A}$  and  $[\gamma\text{-}^{35}\text{S}]\text{ATP}\gamma\text{S}$  binding to cardiac plasma membranes. Experiments were performed as described in the legend of Fig. 2. The data were analyzed by LIGAND [29] and are displayed as Scatchard plots. (A) Scatchard analysis of  $\text{Ap}_4\text{A}$  binding data. The solid line represents the Scatchard parameters generated from linear regression analysis. (B) Scatchard analysis of  $\text{ATP}\gamma\text{S}$  binding data. The dashed line represents the line generated by the apparent  $K_d$  derived from LIGAND after subtracting non-specific binding.

showed a non-linear relationship for  $\text{ATP}\gamma\text{S}$  (Fig. 3B) which suggests there are either two classes of binding sites for  $\text{ATP}\gamma\text{S}$  or there are both specific high affinity binding sites and non-specific binding sites. When using the LIGAND program the analysis is dominated by high affinity interactions. Due to the weighted analysis, the apparent  $\text{ATP}\gamma\text{S}$   $K_d$  value has an upper limit value of  $0.03\text{ }\mu\text{M}$  for the high affinity site and an apparent  $B_{\text{max}}$  of  $99\text{ pmoles mg}^{-1}$  of membrane protein (Table 1).

Equilibrium binding parameters were also determined by performing homologous and heterologous competition studies of  $[\alpha\text{-}^{32}\text{P}]\text{Ap}_4\text{A}$  and  $[\gamma\text{-}^{35}\text{S}]\text{ATP}\gamma\text{S}$

binding using non-radiolabeled  $\text{Ap}_4\text{A}$ ,  $\text{ATP}\gamma\text{S}$ ,  $\alpha,\beta\text{-MeATP}$  and adenosine. The ability of non-radiolabeled  $\text{Ap}_4\text{A}$ ,  $\text{ATP}\gamma\text{S}$  and  $\alpha,\beta\text{-MeATP}$  to inhibit  $[\alpha\text{-}^{32}\text{P}]\text{Ap}_4\text{A}$  binding is presented in Fig. 4A. Variable amounts of non-radiolabeled nucleotides and a fixed amount of  $[\alpha\text{-}^{32}\text{P}]\text{Ap}_4\text{A}$  were incubated with plasma membranes for 15 min at  $20^\circ\text{C}$ . As expected, non-radiolabeled  $\text{Ap}_4\text{A}$  effectively competes with  $[\alpha\text{-}^{32}\text{P}]\text{Ap}_4\text{A}$  for binding sites. Non-radiolabeled  $\text{ATP}\gamma\text{S}$  competed as effectively as did non-radiolabeled  $\text{Ap}_4\text{A}$ . However, the  $\text{P}_{2\text{X}}$  agonist,  $\alpha,\beta\text{-MeATP}$ , was not an effective competitor of  $[\alpha\text{-}^{32}\text{P}]\text{Ap}_4\text{A}$  binding by at least two orders of magnitude.

The ability of non-radiolabeled  $\text{Ap}_4\text{A}$ ,  $\text{ATP}\gamma\text{S}$ ,  $\alpha,\beta\text{-MeATP}$  to compete for  $[\gamma\text{-}^{35}\text{S}]\text{ATP}\gamma\text{S}$  binding is presented in Fig. 4B. Variable amounts of non-radiolabeled nucleotides and a fixed amount of  $[\gamma\text{-}^{35}\text{S}]\text{ATP}\gamma\text{S}$  were incubated with plasma membranes for 15 min at  $20^\circ\text{C}$ . Non-radiolabeled  $\text{ATP}\gamma\text{S}$ , as expected, effectively competes for  $[\gamma\text{-}^{35}\text{S}]\text{ATP}\gamma\text{S}$  binding sites. However, non-radiolabeled  $\text{Ap}_4\text{A}$  was not an effective competitor of  $[\gamma\text{-}^{35}\text{S}]\text{ATP}\gamma\text{S}$  binding. In fact  $1\text{ mM}$   $\text{Ap}_4\text{A}$  inhibits only 60% of  $[\gamma\text{-}^{35}\text{S}]\text{ATP}\gamma\text{S}$  binding. This is in contrast to the reverse experiment in which non-radiolabeled  $\text{ATP}\gamma\text{S}$  effectively inhibited  $[\alpha\text{-}^{32}\text{P}]\text{Ap}_4\text{A}$  binding (Fig. 4A).  $\alpha,\beta\text{-MeATP}$  was also not an effective competitor of  $[\gamma\text{-}^{35}\text{S}]\text{ATP}\gamma\text{S}$  binding with only 60% inhibition at a concentration of  $1\text{ mM}$ . These data are consistent with the presence of a second class of low affinity binding sites for  $\text{ATP}\gamma\text{S}$  which is not effectively competed for by  $\text{Ap}_4\text{A}$  or  $\alpha,\beta\text{-MeATP}$ .

The  $\text{P}_{2\text{X}}$  purinoceptor agonist  $\alpha,\beta\text{-MeATP}$  did not effectively compete with either  $[\alpha\text{-}^{32}\text{P}]\text{Ap}_4\text{A}$  (Fig. 4A) or  $[\gamma\text{-}^{35}\text{S}]\text{ATP}\gamma\text{S}$  (Fig. 4B) binding. In addition adenosine did not compete with either  $[\alpha\text{-}^{32}\text{P}]\text{Ap}_4\text{A}$  or  $[\gamma\text{-}^{35}\text{S}]\text{ATP}\gamma\text{S}$  binding at concentrations up to  $10\text{ mM}$  (data not shown). These data are consistent with neither the high nor low affinity binding sites being a  $\text{P}_{2\text{X}}$  or  $\text{P}_1$  receptor.

Computer analyses of all homologous and heterologous displacement studies were fitted simultaneously with LIGAND and predicted the presence of one high affinity binding site for both  $\text{Ap}_4\text{A}$  and  $\text{ATP}\gamma\text{S}$  and an additional low affinity binding site for  $\text{ATP}\gamma\text{S}$ . At the high affinity binding site the apparent  $K_d$  values for  $\text{Ap}_4\text{A}$  and  $\text{ATP}\gamma\text{S}$  are  $0.08\text{ }\mu\text{M}$  and  $0.04\text{ }\mu\text{M}$ , respectively (Table 1). Non-specific

Table 1  
 $K_d$  values for nucleotide binding to cardiac plasma membranes

Nucleotide	Scatchard analysis <sup>a</sup>	Competition analysis <sup>b</sup>	
	$K_d$ high affinity site ( $\mu$ M)	$K_d$ high affinity site ( $\mu$ M)	$K_d$ low affinity site ( $\mu$ M)
Ap <sub>4</sub> A	0.05	0.08	—
ATP $\gamma$ S	0.03 <sup>c</sup>	0.04	1.0
$\alpha$ , $\beta$ -MeATP	nd <sup>d</sup>	3.0	—

<sup>a</sup>2.5  $\mu$ g of plasma membranes were incubated with varying amounts of either [ $\alpha$ -<sup>32</sup>P]Ap<sub>4</sub>A (specific activity 6000–9000 cpm/pmole) or [ $\gamma$ -<sup>35</sup>S]ATP $\gamma$ S (specific activity 6000–9000 cpm/pmole) in a final volume of 0.1 ml as described in the legend of Fig. 2. Saturation binding curves were fitted directly to raw cpm data and analyzed by the program LIGAND as described in the text.

<sup>b</sup>2.5  $\mu$ g of plasma membranes were incubated with either 0.5  $\mu$ M [ $\alpha$ -<sup>32</sup>P]Ap<sub>4</sub>A (specific activity 6000–9000 cpm/pmole) or 0.9  $\mu$ M [ $\gamma$ -<sup>35</sup>S]ATP $\gamma$ S (specific activity 6000–9000 cpm/pmole) and varying amounts of competing non-radiolabeled ligand (0.4 nM–1.0 mM) in a final volume of 0.1 ml as described in the legend of Fig. 4. Data from all homologous and heterologous displacement experiments were simultaneously fitted and analyzed by the program LIGAND as described in the text.

<sup>c</sup>Upper limit  $K_d$  value for the high affinity site.

<sup>d</sup>Equilibrium binding parameters were not determined by this method.

binding ratios of 0.001 and 0.0007 were calculated for Ap<sub>4</sub>A and ATP $\gamma$ S, respectively, indicating that less than 0.1% of the total high affinity binding was due to non-specific interactions. The apparent  $K_d$  value for the low affinity ATP $\gamma$ S site is 1.0  $\mu$ M (Table 1); however, the non-specific binding ratio of 0.012 is relatively high compared to those for the high affinity site. These data are consistent with Ap<sub>4</sub>A and ATP $\gamma$ S binding to the same high affinity site on cardiac plasma membranes.

### 3.4. Identification of the Ap<sub>4</sub>A receptor by photocrosslinking [ $\alpha$ -<sup>32</sup>P]8-N<sub>3</sub>Ap<sub>4</sub>A to plasma membranes

To identify the Ap<sub>4</sub>A receptor, 5  $\mu$ g of plasma membranes were incubated with [ $\alpha$ -<sup>32</sup>P]8-N<sub>3</sub>Ap<sub>4</sub>A for 30 min at 20°C prior to UV crosslinking. SDS-PAGE followed by Western transfer and autoradiography revealed [ $\alpha$ -<sup>32</sup>P]8-N<sub>3</sub>Ap<sub>4</sub>A photolabeling of a 50 kDa and a smaller amount of a 30 kDa polypeptide (Fig. 5). Since we have previously shown that the 30 kDa polypeptide is a consequence of artifactual receptor proteolysis [26], these data are consistent with Ap<sub>4</sub>A binding to a 50 kDa polypeptide on purified cardiac plasma membranes.

The hydrolysis of ATP by cardiac plasma membranes prevented the use of ATP in radioligand binding studies. In an attempt to determine the interactions of ATP with the cardiac Ap<sub>4</sub>A receptor, studies using immunoaffinity purified Ap<sub>4</sub>A receptor were

performed. The Ap<sub>4</sub>A receptor polypeptide was immunoaffinity purified with an anti-Ap<sub>4</sub>A receptor mAb (mAb TL 4) that we have raised against the mouse cardiac receptor [23]. The immunoaffinity purified receptor was photolabeled with varying concentrations of [ $\alpha$ -<sup>32</sup>P]8-N<sub>3</sub>Ap<sub>4</sub>A, followed by SDS-PAGE, Western transfer and autoradiography. As shown in Fig. 6, photolabeling with [ $\alpha$ -<sup>32</sup>P]8-N<sub>3</sub>Ap<sub>4</sub>A was linear for concentrations of 5–20  $\mu$ M and reached a plateau at 20  $\mu$ M.

The ability of non-radiolabeled Ap<sub>4</sub>A, ATP $\gamma$ S and ATP to inhibit [ $\alpha$ -<sup>32</sup>P]8-N<sub>3</sub>Ap<sub>4</sub>A photocrosslinking to purified polypeptide fractions is shown in Fig. 7. Ligand specificity of the Ap<sub>4</sub>A receptor was determined by incubating variable amounts of non-radiolabeled nucleotides and a fixed amount of [ $\alpha$ -<sup>32</sup>P]8-N<sub>3</sub>Ap<sub>4</sub>A prior to UV crosslinking, SDS-PAGE, Western transfer and autoradiography. As expected both Ap<sub>4</sub>A and ATP $\gamma$ S effectively inhibit [ $\alpha$ -<sup>32</sup>P]8-N<sub>3</sub>Ap<sub>4</sub>A crosslinking to the receptor polypeptides. However, ATP is significantly less effective at competing for [ $\alpha$ -<sup>32</sup>P]8-N<sub>3</sub>Ap<sub>4</sub>A (Fig. 7). The estimated IC<sub>50</sub> values for ATP $\gamma$ S, Ap<sub>4</sub>A and ATP are 56  $\mu$ M, 158  $\mu$ M and 2500  $\mu$ M, respectively. Higher concentrations of Ap<sub>4</sub>A and ATP $\gamma$ S were required for competing with [ $\alpha$ -<sup>32</sup>P]8-N<sub>3</sub>Ap<sub>4</sub>A photocrosslinking (Fig. 7) than with [<sup>32</sup>P]Ap<sub>4</sub>A binding to plasma membranes (Fig. 4). The higher concentration of non-photoactive ligand that is required to inhibit photolabeling can be explained on the basis of reversible binding of the non-photoactive ligand and the covalent

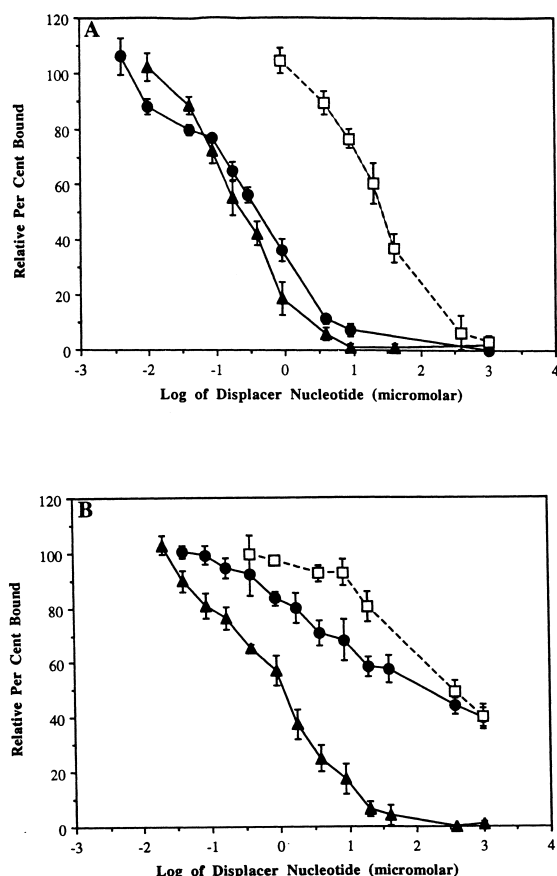


Fig. 4. Inhibition of  $[\alpha\text{-}^{32}\text{P}]\text{Ap}_4\text{A}$  and  $[\gamma\text{-}^{35}\text{S}]\text{ATP}\gamma\text{S}$  binding to cardiac plasma membranes by unlabeled  $\text{Ap}_4\text{A}$ ,  $\text{ATP}\gamma\text{S}$  and  $\alpha,\beta\text{-MeATP}$ . The binding assay is described in the text. (A) 2.5  $\mu\text{g}$  of plasma membranes were incubated with 0.5  $\mu\text{M}$   $[\alpha\text{-}^{32}\text{P}]\text{Ap}_4\text{A}$  (specific activity 6000–9000 cpm/pmole) and varying concentrations of non-radiolabeled ligand for 15 min at 20°C. ●,  $\text{Ap}_4\text{A}$ ; ▲,  $\text{ATP}\gamma\text{S}$ ; □,  $\alpha,\beta\text{-MeATP}$ . (B) 2.5  $\mu\text{g}$  of plasma membranes were incubated with 0.9  $\mu\text{M}$   $[\gamma\text{-}^{35}\text{S}]\text{ATP}\gamma\text{S}$  (specific activity 6000–9000 cpm/pmole) and varying concentrations of non-radiolabeled nucleotide for 15 min at 20°C. ●,  $\text{Ap}_4\text{A}$ ; ▲,  $\text{ATP}\gamma\text{S}$ ; □,  $\alpha,\beta\text{-MeATP}$ . Results are expressed as averages of at least six experiments in duplicate (12 total data points). Error bars are shown as standard deviations.

lent binding of the photoactive ligand [31]. In addition, similar observations have been made by other investigators who found that excess cAMP and  $\text{Ap}_4\text{A}$  were required to inhibit photoincorporation of 8- $\text{N}_3\text{-cAMP}$  and 8- $\text{N}_3\text{Ap}_4\text{A}$ , respectively [31,32].

To ensure that the immunoaffinity purified  $\text{Ap}_4\text{A}$  receptor did not contain  $\text{Ap}_4\text{A}$  hydrolyases or ATPases, immunoaffinity purified receptor was incubated with  $[\text{P}]\text{Ap}_4\text{A}$ ,  $[\text{P}]\text{ATP}$  or  $[\text{S}]\text{ATP}\gamma\text{S}$  for 30 min at 20°C. Aliquots were subjected to

TLC followed by autoradiography. Greater than 90% of radiolabeled  $[\text{P}]\text{Ap}_4\text{A}$ ,  $[\text{P}]\text{ATP}$  and  $[\text{S}]\text{ATP}\gamma\text{S}$  co-migrates with non-radiolabeled  $\text{Ap}_4\text{A}$ ,  $\text{ATP}$  and  $\text{ATP}\gamma\text{S}$ , respectively (data not shown). Furthermore, the design of  $[\alpha\text{-}^{32}\text{P}]\text{8-N}_3\text{Ap}_4\text{A}$  is such that no likely degradation products can contain both radiolabel and photoactive azido group, thus ensuring that any labeling is due to the intact molecule. These data are consistent with  $\text{Ap}_4\text{A}$  and  $\text{ATP}\gamma\text{S}$  specifically interacting with the cardiac plasma membrane  $\text{Ap}_4\text{A}$  receptor but with  $\text{ATP}$  having a low affinity for this receptor.

#### 4. Discussion

In different tissues and cell types  $\text{Ap}_4\text{A}$  has been shown to interact with  $\text{P}_{2Y}$ ,  $\text{P}_{2X}$ , as well as  $\text{P}_{2D}$  purinoceptors [1,2,17,18,21,22,24,25]. Furthermore, evidence from physiological and molecular studies suggests that a heterogeneous population of purinoceptors exists within cardiac tissue [24,25]. However, the relationship of  $\text{Ap}_4\text{A}$  to the various purinoceptors in cardiac plasma membranes is not clear. The work presented in this communication is consistent with  $\text{Ap}_4\text{A}$  and  $\text{ATP}\gamma\text{S}$  interacting with a homogeneous population of receptors on cardiac plasma membranes and that  $\text{ATP}$  has a low affinity for the  $\text{Ap}_4\text{A}$  receptor.

The presence of ectonucleotidases that rapidly hy-

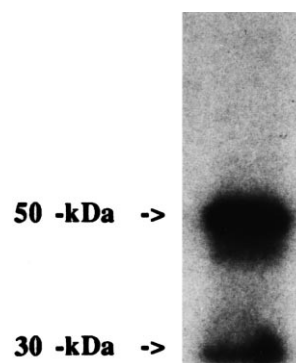


Fig. 5. SDS-PAGE and autoradiography of  $[\alpha\text{-}^{32}\text{P}]\text{8-N}_3\text{Ap}_4\text{A}$  photolabeled cardiac plasma membrane. Plasma membrane was isolated as described in the text. 5.0  $\mu\text{g}$  of plasma membrane were incubated in 30  $\mu\text{l}$  of assay buffer with 1.2 nM  $[\alpha\text{-}^{32}\text{P}]\text{8-N}_3\text{Ap}_4\text{A}$  (specific activity  $4.8 \times 10^7$  cpm/pmole) for 30 min at 20°C prior to UV crosslinking and SDS-PAGE as described in the text. Molecular weights are denoted by the arrows.



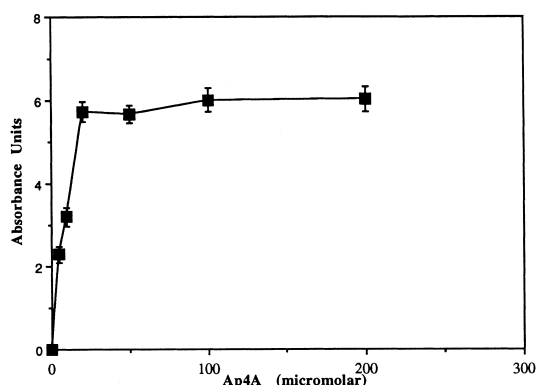


Fig. 6. SDS-PAGE and autoradiography of  $[\alpha\text{-}^{32}\text{P}]\text{8-N}_3\text{Ap}_4\text{A}$  photolabeled immunoaffinity purified  $\text{Ap}_4\text{A}$  receptor 50 kDa polypeptide. 5.0  $\mu\text{g}$  of immunoaffinity purified receptor were incubated in 30  $\mu\text{l}$  of assay buffer with varying amounts of  $[\alpha\text{-}^{32}\text{P}]\text{8-N}_3\text{Ap}_4\text{A}$  (specific activity 1200–1800 cpm/pmol) for 30 min at 20°C prior to UV crosslinking and SDS-PAGE as described in the text. Photolabeling was detected by autoradiography and quantified by densitometry as described in the text. Absorbance units are equal to  $A_{533} \times \text{mm}^2$ . The results are expressed as an average of three different experiments in triplicate (nine total data points). Error bars are shown as standard deviations.

hydrolyze ATP and adenylated dinucleotides may preclude direct investigations into the action of these nucleotides on many tissues and cells. Hulme and Birdsall have suggested that greater than 75% of the radioligand must remain intact to obtain reliable equilibrium binding parameters [33]. Optimal binding conditions required a 15 min incubation at 20°C to obtain equilibrium. Following a 15 min incubation, 80.2%, 91.7%, 100% and 33.3% of the radiolabeled  $\text{Ap}_4\text{A}$ ,  $\text{ATP}\gamma\text{S}$ ,  $\alpha,\beta\text{-MeATP}$  and ATP migrated with control standards, respectively (Fig. 1). These data demonstrate that  $\text{Ap}_4\text{A}$ ,  $\text{ATP}\gamma\text{S}$ ,  $\alpha,\beta\text{-MeATP}$  meet the Hulme and Birdsall criteria, while using ATP in receptor-ligand studies would be biased by unknown concentrations of hydrolytic products.

Considering the rapid hydrolysis of ATP by cardiac plasma membranes two synthetic ATP analogs were selected for use in radioligand binding studies. We chose  $\text{ATP}\gamma\text{S}$ , a potent  $\text{P}_{2Y}$  agonist [34], and  $\alpha,\beta\text{-MeATP}$ , a potent  $\text{P}_{2X}$  agonist [18], to investigate mononucleotide interactions with the  $\text{Ap}_4\text{A}$  receptor on cardiac plasma membranes. Homologous and heterologous competition studies carried out with  $[\alpha\text{-}^{32}\text{P}]\text{Ap}_4\text{A}$  and  $[\gamma\text{-}^{35}\text{S}]\text{ATP}\gamma\text{S}$  are consistent with  $\text{Ap}_4\text{A}$  interacting with only a single class of high

affinity binding site while  $\text{ATP}\gamma\text{S}$  interacts with this same class of high affinity sites and a second low affinity site (Fig. 4 and Table 1). Apparent  $K_d$  values for the high affinity site obtained from competition studies for  $\text{Ap}_4\text{A}$  and  $\text{ATP}\gamma\text{S}$  are in good agreement with the values obtained from Scatchard analysis (Table 1). Computer curve-fitting of both competition and Scatchard analysis is consistent with  $\text{Ap}_4\text{A}$  binding to a homogeneous population of receptors on cardiac plasma membranes.

The use of multiple radioligands and two independent methods for determining equilibrium binding parameters not only strengthens the notion of a single high affinity  $\text{Ap}_4\text{A}$  receptor but also allows for the observation of a two binding site model for  $\text{ATP}\gamma\text{S}$ . Although  $\text{Ap}_4\text{A}$  and  $\text{ATP}\gamma\text{S}$  both effectively competed for  $[\alpha\text{-}^{32}\text{P}]\text{Ap}_4\text{A}$  binding,  $\text{Ap}_4\text{A}$  only competed with 60% of the total  $[\gamma\text{-}^{35}\text{S}]\text{ATP}\gamma\text{S}$  binding (Fig. 4B). These data are consistent with the presence of at least two binding sites for  $\text{ATP}\gamma\text{S}$  on cardiac plasma membranes.

The apparent  $K_d$  values of 0.03 and 0.04  $\mu\text{M}$  for  $\text{ATP}\gamma\text{S}$  (Table 1) are similar to the values reported for  $\text{ATP}\gamma\text{S}$  binding to  $\text{P}_{2Y}$  receptors on endothelial

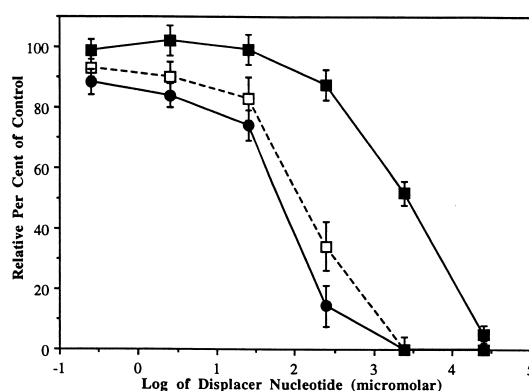


Fig. 7. Inhibition of  $[\alpha\text{-}^{32}\text{P}]\text{8-N}_3\text{Ap}_4\text{A}$  binding to the immunoaffinity purified  $\text{Ap}_4\text{A}$  receptor 50 kDa polypeptide by unlabeled  $\text{Ap}_4\text{A}$ ,  $\text{ATP}\gamma\text{S}$  and ATP. 5.0  $\mu\text{g}$  of immunoaffinity purified receptor were incubated in 30  $\mu\text{l}$  of assay buffer with 25  $\mu\text{M}$   $[\alpha\text{-}^{32}\text{P}]\text{8-N}_3\text{Ap}_4\text{A}$  (specific activity 1200–1800 cpm/pmol) and various concentrations of non-radiolabeled  $\text{Ap}_4\text{A}$ ,  $\text{ATP}\gamma\text{S}$ , or ATP for 30 min at 20°C prior to UV crosslinking and SDS-PAGE as described in the text. Photolabeling was detected by autoradiography and quantified by densitometry as described in the text. Absorbance units are equal to  $A_{533} \times \text{mm}^2$ .  $\square$ ,  $\text{Ap}_4\text{A}$ ;  $\bullet$ ,  $\text{ATP}\gamma\text{S}$ ;  $\blacksquare$ , ATP. The results are expressed as an average of three different experiments in triplicate (nine total data points). Error bars are shown as standard deviations.

membranes (0.01  $\mu\text{M}$ ) [35] and for ATP $\alpha\text{S}$  binding to  $\text{P}_{2\text{Y}}$  receptors on liver plasma membranes (0.19  $\mu\text{M}$ ) [36,37].  $\text{Ap}_4\text{A}$  binds to a single class of  $\text{P}_{2\text{Y}}$  binding sites on liver plasma membranes with an apparent  $K_{\text{d}}$  value (1.76  $\mu\text{M}$ ) [21] that is about 33-fold higher than the value we obtained from cardiac plasma membranes (Table 1). On the other hand,  $\text{Ap}_4\text{A}$  appears to bind to two classes of binding sites on brain synaptosomes and chromaffin cells with apparent  $K_{\text{d}}$  values of 0.1 nM and 0.08 nM for the high affinity sites and apparent  $K_{\text{i}}$  values of 0.57  $\mu\text{M}$  and 0.13  $\mu\text{M}$  for the low affinity sites, respectively [22,38]. These data suggest that there may be heterogeneity of  $\text{Ap}_4\text{A}$  binding sites in the various tissues.

Competition studies indicate that  $\text{Ap}_4\text{A}$  and ATP $\gamma\text{S}$  have similar binding affinities for the high affinity site while  $\alpha,\beta\text{-MeATP}$  and adenosine were ineffective competitors of either  $[\alpha\text{-}^{32}\text{P}]\text{Ap}_4\text{A}$  or  $[\gamma\text{-}^{35}\text{S}]\text{ATP}\gamma\text{S}$ . Other investigators have demonstrated that ATP $\alpha\text{S}$  and  $\alpha,\beta\text{-MeATP}$  bind to different  $\text{P}_{2\text{Y}}$  and  $\text{P}_{2\text{X}}$  purinoceptors on brain synaptosomal membranes, respectively [39]. These data are consistent with the high affinity  $\text{Ap}_4\text{A}$  binding site on cardiac plasma membranes not being a  $\text{P}_{2\text{X}}$  or  $\text{P}_1$  receptor.

Our apparent  $B_{\text{max}}$  value of 66 pmol  $\text{mg}^{-1}$  for the  $\text{Ap}_4\text{A}$  receptor on cardiac plasma membranes is within the range of receptor densities observed for  $\text{Ap}_4\text{A}$  in liver plasma membranes (47 pmol  $\text{mg}^{-1}$ ) [21]. However, the  $\text{Ap}_4\text{A}$  cardiac plasma membrane receptor density is more than three orders of magnitude greater than the  $B_{\text{max}}$  values for the high affinity  $\text{Ap}_4\text{A}$  binding site on brain synaptosomes (16 fmoles  $\text{mg}^{-1}$ ) [22]. These data suggest that there are variations of  $\text{Ap}_4\text{A}$  receptor densities in different tissues.

On purified cardiac plasma membranes  $[\alpha\text{-}^{32}\text{P}]\text{8-N}_3\text{Ap}_4\text{A}$  only photolabeled a 50 and a 30 kDa polypeptide (Fig. 5). Since we have previously shown that the 30 kDa polypeptide is a consequence of artifactual receptor proteolysis [26], these data are consistent with  $\text{Ap}_4\text{A}$  binding to a 50 kDa polypeptide on purified cardiac plasma membranes. However, we have also demonstrated that on isolated cardiac myocytes  $[\alpha\text{-}^{32}\text{P}]\text{8-N}_3\text{Ap}_4\text{A}$  photolabeled only a 42 kDa polypeptide [26]. We have also previously demonstrated that the  $\text{Ap}_4\text{A}$  receptor undergoes at least two proteolytic processing steps, one of which is carried out by a serine protease [1,2,23] and that this

serine protease is required for receptor activation. Since the serine protease is separated from the plasma membrane during plasma membrane purification (unpublished observation), this suggests that the  $\text{Ap}_4\text{A}$  receptor on purified cardiac plasma membranes has not been activated and that the 50 kDa polypeptide represents the  $\text{Ap}_4\text{A}$  receptor prior to processing. The apparent  $K_{\text{d}}$  value for  $\text{Ap}_4\text{A}$  on cardiac plasma membranes (Table 1) is 4-fold higher than the value obtained for activated partially purified cardiac membrane homogenates [2]. Although unactivated, the higher purification of plasma membranes allows for a more accurate estimation of binding affinity than studies with partially purified membrane homogenates. This is evidenced by the 8-fold lower  $K_{\text{d}}$  value obtained for  $\text{Ap}_4\text{A}$  with purified plasma membranes than the  $K_{\text{d}}$  value (0.65  $\mu\text{M}$ ) obtained for unactivated partially purified membrane homogenates [2]. Nevertheless, these data are consistent with  $\text{Ap}_4\text{A}$  interacting with a single 50 kDa polypeptide on cardiac plasma membranes.

A number of  $\text{P}_{2\text{Y}}$  agonists have been shown to have varying effects on  $\text{Ap}_4\text{A}$  binding to membrane receptors. The  $\text{P}_{2\text{Y}}$  agonist ADP $\beta\text{S}$  is an effective competitor of radiolabeled  $\text{Ap}_4\text{A}$  binding to brain synaptosome [22] and chromaffin cell  $\text{P}_{2\text{D}}$  purinoceptors [38]. ATP $\gamma\text{S}$  is nearly as effective as  $\text{Ap}_4\text{A}$  at activating cloned  $\text{P}_{2\text{U}}$  receptors expressed in astrocytoma cells [40]. On the other hand  $\text{Ap}_4\text{A}$  does not compete with the  $\text{P}_{2\text{Y}}$  agonist ATP $\alpha\text{S}$  binding to brain synaptosomes [39] or liver  $\text{P}_{2\text{Y}}$  receptors [36]. These observations suggest that classification of the  $\text{Ap}_4\text{A}$  receptor as a  $\text{P}_{2\text{D}}$  purinoceptor should not be accomplished by only using synthetic ATP analogs because their specificity may be cell and tissue specific. In addition, due to the presence of enzymes on purified cardiac plasma membranes that rapidly hydrolyze ATP (Fig. 1), direct investigations of the action of ATP is precluded. Consequently, a second approach was required to assess the relationship of ATP to the  $\text{Ap}_4\text{A}$  receptor. This was accomplished by photoaffinity labeling studies of the  $\text{Ap}_4\text{A}$  receptor immunoaffinity purified using mAb TL4. Monoclonal antibody TL4 has been shown to interact with part of the  $\text{Ap}_4\text{A}$  binding domain [41]. Both non-labeled ATP $\gamma\text{S}$  and  $\text{Ap}_4\text{A}$  were effective competitors of  $[\alpha\text{-}^{32}\text{P}]\text{8-N}_3\text{Ap}_4\text{A}$  with estimated  $\text{IC}_{50}$  values of 56 and 158  $\mu\text{M}$ , respectively. In contrast, non-labeled

ATP was not an effective inhibitor of [ $\alpha$ - $^{32}\text{P}$ ]8-N<sub>3</sub>Ap<sub>4</sub>A (estimated IC<sub>50</sub> of 2500  $\mu\text{M}$ ) (Fig. 7). These data demonstrate that ATP does not bind in appreciable amounts to the Ap<sub>4</sub>A receptor.

The data presented in this communication are consistent with Ap<sub>4</sub>A interacting with a homogeneous population of receptors on cardiac plasma membranes and with ATP having a low affinity for this receptor. These data also support our previous observations that the cardiac Ap<sub>4</sub>A receptor is a unique dipurinoceptor which is highly specific for adenylated dinucleotides [1,2]. However, final placement of the cardiac Ap<sub>4</sub>A receptor as a distinct P<sub>2</sub> purinoceptor subclass must await the isolation and sequencing of Ap<sub>4</sub>A receptor full length cDNA clones.

### Acknowledgements

The authors would like to thank Drs. Gary Powell and James Zimmerman of Clemson University for critically evaluating this manuscript. This research was supported in part by USDA NRICG 96-35204-3669, Greenville Hospital System/Clemson University Cooperative and South Carolina Experiment Station Grant SC01630.

### References

- [1] J. Walker, T. Lewis, E.P. Pivorun, R.H. Hilderman, Activation of the mouse heart adenosine 5',5'''-P<sup>1</sup>,P<sup>4</sup>-tetraphosphate receptor, *Biochemistry* 32 (1993) 1264–1269.
- [2] R.H. Hilderman, J.E. Lilien, J.K. Zimmerman, D.H. Tate, M.A. Dimmick, G.B. Jones, Adenylated dinucleotide binding to the adenosine 5',5'''-tetraphosphate mouse heart receptor, *Biochem. Biophys. Res. Commun.* 200 (1994) 749–755.
- [3] H. Flodgaard, H. Klenow, Abundant amounts of diadenosine 5',5'''-P<sup>1</sup>,P<sup>4</sup>-tetraphosphate (Ap<sub>4</sub>A) are present and releasable, but metabolically inactive in human platelets, *Biochem. J.* 208 (1982) 737–741.
- [4] H. Schluter, E. Offers, G. Bruggemann, M. van der Giet, M. Tepel, E. Nordhoff, M. Karas, C. Spieker, H. Witzel, W. Zidek, Diadenosine phosphates and the physiological control of blood pressure, *Nature* 367 (1994) 186–188.
- [5] A. Rodriguez Del Castillo, M. Torres, E.G. Delicado, M.Y. Miras-Portugal, Subcellular distribution studies of diadenosine polyphosphates-Ap<sub>4</sub>A and Ap<sub>5</sub>A in bovine adrenal medulla: presence in chromaffin granules, *J. Neurochem.* 51 (1988) 1696–1703.
- [6] J. Pintor, P. Rotlan, M. Torres, M.T. Miras-Portugal, Characterization and quantification of diadenosine hexaphosphate in chromaffin cells: granular storage and secretagogue-induced release, *Anal. Biochem.* 200 (1992) 296–300.
- [7] J. Luthje, A. Ogilvie, Catabolism of Ap<sub>4</sub>A and Ap<sub>3</sub>A in whole blood. The dinucleotides are long-lived signal molecules in the blood ending up as intracellular ATP in the erythrocytes, *Eur. J. Biochem.* 173 (1988) 241–245.
- [8] R.H. Hilderman, D.B. Wiest, B. Blackwell, E.E. Hodgson, M.M. Swindle, The role of P<sup>1</sup>,P<sup>4</sup>-diadenosine 5'-tetraphosphate as a vasodilator, *Am. J. Hypertens.* 10 (1997) 94A.
- [9] Y. Kikuta, A. Sekine, S. Tezuka, K. Okada, T. Yamaura, H. Nakajima, Intravenous diadenosine tetraphosphate in dogs. Cardiovascular effects and influence on blood gases, *Acta Anaesthesiol. Scand.* 38 (1994) 284–288.
- [10] U. Pohl, A. Ogilvie, D. Lamontagne, R.P. Busse, Potent effects of Ap<sub>3</sub>A and Ap<sub>4</sub>A on coronary resistance and autacoid release of intact rabbit hearts, *Am. J. Physiol.* 260 (1991) H1692–H1697.
- [11] R.H. Hilderman, E.F. Christensen, P<sup>1</sup>,P<sup>4</sup>-Diadenosine 5'-tetraphosphate induces nitric oxide release from bovine aortic endothelial cells, *FEBS Lett.* 427 (1988) 320–324.
- [12] L. Gasmi, A.G. McLennan, M.J. Fisher, Priming of the respiratory burst of human neutrophils by the diadenosine polyphosphates Ap<sub>4</sub>A and Ap<sub>3</sub>A: role of intracellular calcium, *Biochem. Biophys. Res. Commun.* 202 (1993) 218–224.
- [13] J. Luthje, J. Baringer, A. Ogilvie, Effects of diadenosine triphosphate (Ap<sub>3</sub>A) and diadenosine tetraphosphate (Ap<sub>4</sub>A) on platelet aggregation in unfractionated human blood, *Blut* 51 (1985) 405–413.
- [14] P.C. Zamecnik, B. Kim, M.J. Gao, G. Taylor, M. Blackburn, Analogues of diadenosine 5',5'''-P<sup>1</sup>,P<sup>4</sup>-tetraphosphate (Ap<sub>4</sub>A) as potential anti-platelet-aggregation agents, *Proc. Natl. Acad. Sci. USA* 89 (1992) 2370–2373.
- [15] E. Castro, M. Torres, M.T. Miras-Portugal, M.P. Gonzalez, Effect of diadenosine polyphosphates on catecholamine secretion from isolated chromaffin cells, *Br. J. Pharmacol.* 100 (1990) 360–364.
- [16] K.M. Craik, A.G. McLennan, M.J. Fisher, Adenine dinucleotide-mediated activation of glycogen phosphorylase in isolated liver cells, *Cell. Signals* 5 (1993) 89–96.
- [17] T.D. Westfall, C.A. McIntyre, S. Obeid, J. Bowes, C. Kennedy, P. Sneddon, The interaction of diadenosine polyphosphates with P<sub>2X</sub>-receptors in the guinea-pig isolated vas deferens, *Br. J. Pharmacol.* 121 (1997) 57–62.
- [18] X. Bo, B. Fisher, M. Maillard, K.A. Jacobson, G. Burnstock, Comparative studies on the affinities of ATP derivatives for P<sub>2X</sub>-purinoceptors in rat urinary bladder, *Br. J. Pharmacol.* 112 (1994) 1151–1159.
- [19] E. Castro, J. Pintor, M.Y. Miras-Portugal, Ca<sup>2+</sup>-stores mobilization by diadenosine tetraphosphate, Ap<sub>4</sub>A, through a putative P<sub>2Y</sub> purinoceptor in adrenal chromaffin cells, *Br. J. Pharmacol.* 106 (1992) 833–837.
- [20] R.P. Sen, E.G. Delicado, E. Castro, M.T. Miras-Portugal, Effect of P<sub>2Y</sub> agonists on adenosine transport in cultured chromaffin cells, *J. Neurochem.* 60 (1993) 613–619.

- [21] M. Edgecombe, G. McLennan, M.J. Fisher, Characterization of the binding of diadenosine 5',5'''-P<sup>1</sup>,P<sup>4</sup>-tetrphosphate (Ap<sub>4</sub>A) to rat liver cell membranes, *Biochem. J.* 314 (1996) 687–693.
- [22] J. Pintor, M.A. Díaz-Ray, M.T. Miras-Portugal, Ap<sub>4</sub>A and ADPβS binding to P<sub>2</sub> purinoceptors present on rat brain synaptic terminals, *Br. J. Pharmacol.* 108 (1993) 1094–1099.
- [23] J. Walker, R.H. Hilderman, Identification of a serine protease which activates the mouse heart adenosine 5',5'''-P<sup>1</sup>,P<sup>4</sup>-tetrphosphate receptor, *Biochemistry* 32 (1993) 3119–3123.
- [24] M. Garcia-Guzman, F. Soto, B. Laube, W. Stühmer, Molecular cloning and functional expression of a novel rat heart P<sub>2X</sub> purinoceptor, *FEBS Lett.* 388 (1996) 123–127.
- [25] Y. Tokuyama, M. Hara, E.M.C. Jones, Z. Fan, G.I. Bell, Cloning of rat and mouse P<sub>2Y</sub> purinoceptors, *Biochem. Biophys. Res. Commun.* 211 (1995) 211–218.
- [26] J. Walker, P. Bossman, B. Lackey, J.K. Zimmerman, M.A. Dimmick, R.H. Hilderman, The adenosine 5',5'''-P<sup>1</sup>,P<sup>4</sup>-tetrphosphate receptor is at the cell surface, *Biochemistry* 32 (1993) 14009–14014.
- [27] R.H. Hilderman, Characterization of a homogenous arginyl-lysyl-tRNA synthetase complex: zinc and AMP dependent synthesis of Ap<sub>4</sub>A, *Biochemistry* 32 (1983) 14009–14014.
- [28] R.H. Hilderman, M. Martin, J.K. Zimmerman, E.P. Pivorum, Identification of a unique adenosine 5',5'''-P<sup>1</sup>,P<sup>4</sup>-tetrphosphate receptor, *J. Biol. Chem.* 266 (1991) 6915–6918.
- [29] P.J. Munson, D. Rodbard, LIGAND: a versatile computerized approach for characterization of ligand-binding systems, *Anal. Biochem.* 107 (1980) 220–239.
- [30] M.M. Bradford, A rapid and sensitive method for the quantitation of microgram quantities of protein utilizing the principle of protein-dye binding, *Anal. Biochem.* 72 (1976) 248–304.
- [31] A.H. Pomerantz, S.A. Rudolph, B.E. Haley, P. Greengard, Photoaffinity labeling of a protein kinase from bovine brain with 8-azidoadenosine 3',5'-monophosphate, *Biochemistry* 14 (1975) 3858–3862.
- [32] M. Baxi, A.G. McLennan, J.K. Vishwanatha, Characterization of the HeLa cell DNA polymerase α-associated Ap<sub>4</sub>A binding protein by photoaffinity labeling, *Biochemistry* 33 (1994) 14601–14607.
- [33] E.C. Hulme, N.J.M., Birdsall, *Receptor-Ligand Interactions: a Practical Approach*, Oxford University Press, New York, 1992.
- [34] S. Motte, D. Communi, S. Pirotton, J.-M. Boeynaems, Involvement of multiple receptors in the actions of extracellular ATP: the example of vascular endothelial cells, *Int. J. Biochem. Cell Biol.* 27 (1995) 1–7.
- [35] S. Motte, S. Swillens, J.M. Boeynaems, Evidence that most high-affinity ATP binding sites on aortic endothelial cells and membranes do not correspond to P<sub>2</sub> receptors, *Eur. J. Pharmacol.* 307 (1996) 201–209.
- [36] S. Keppans, A. Vandekerckhove, H. De Wulf, Characterization of purinoceptors present on human liver plasma membranes, *FEBS Lett.* 248 (1989) 137–140.
- [37] S. Keppens, H. De Wulf, Characterization of the liver P<sub>2</sub>-purinoceptor involved in the activation of glycogen phosphorylase, *Biochem. J.* 240 (1986) 367–371.
- [38] J. Pintor, M. Torres, E. Castro, M.T. Miras-Portugal, Characterization of diadenosine tetrphosphate (Ap<sub>4</sub>A) binding sites in cultured chromaffin cells: evidence for a P<sub>2Y</sub> site, *Br. J. Pharmacol.* 103 (1991) 1980–1984.
- [39] R. Schafer, G. Reiser, Characterization of [<sup>35</sup>S]-ATPαS and [<sup>3</sup>H]-α,β MeATP binding sites in rat brain cortical synaptosomes: regulation of ligand binding by divalent cations, *Br. J. Pharmacol.* 121 (1997) 913–922.
- [40] E.R. Lazarowski, W.C. Watt, M.J. Stutts, R.C. Boucher, T.K. Harden, Pharmacological selectivity of the cloned human P<sub>2U</sub> purinoceptor: potent activation by diadenosine tetrphosphate, *Br. J. Pharmacol.* 116 (1995) 1619–1627.
- [41] G. Liu, R.B. Bryant, R.H. Hilderman, Isolation of a tripeptide from a random phage peptide library that inhibits adenosine 5',5'''-P<sup>1</sup>,P<sup>4</sup>-tetrphosphate binding to its receptor, *Biochemistry* 35 (1996) 197–201.